

Hysteretic Energy Demand in SDOF Structures Subjected to an Earthquake Excitation: Analytical and Empirical Results

Taner UÇAR^{*1}, Onur MERTER²

¹Dokuz Eylül Üniversitesi, Mimarlık Fakültesi, Mimarlık Bölümü, 35160, İzmir

²Uşak Üniversitesi, Mühendislik Fakültesi, İnşaat Mühendisliği Bölümü, 64000, Uşak

(Alınış / Received: 14.06.2017, Kabul / Accepted: 27.02.2018, Online Yayınlanma / Published Online: 11.04.2018)

Keywords

Earthquake ground motion,
Hysteretic energy,
Input energy,
NLTH analysis,
SDOF system,
Hysteretic energy to input
energy ratio

Abstract: In energy-based seismic design approach, earthquake ground motion is considered as an energy input to structures. The earthquake input energy is the total of energy components such as kinetic energy, damping energy, elastic strain energy and hysteretic energy, which contributes the most to structural damage. In literature, there are many empirical formulas based on the hysteretic model, damping ratio and ductility in order to estimate hysteretic energy, whereas they do not directly consider the ground motion characteristics. This paper uses nonlinear time history (NLTH) analysis for energy calculations and presents the distribution of earthquake input energy and hysteretic energy of single-degree-of-freedom (SDOF) systems over the ground motion duration. Seven real earthquakes recorded on the same soil profile and three different bilinear SDOF systems having constant ductility ratio and different natural periods are selected to perform NLTH analyses. As results of nonlinear dynamic analyses, input and hysteretic energies per unit masses are graphically obtained. The hysteretic energy to input energy ratio (E_H/E_I) is investigated, as well as the ratio of other energy components to energy input. E_H/E_I ratios of NLTH analysis are compared to the results of empirical approximations related E_H/E_I ratio and a reasonable agreement is observed. The average of E_H/E_I ratio is found to be between 0.468 and 0.488 meaning nearly half of the earthquake energy input is dissipated through the hysteretic behavior.

Deprem Etkisindeki TSD Yapılarda Histeretik Enerji Talebi: Analitik ve Ampirik Sonuçlar

Anahtar Kelimeler

Deprem yer hareketi,
Histeretik enerji,
Giren enerji,
Zaman tanım alanında
doğrusal olmayan analiz,
TSD sistem,
Histeretik enerji/toplam
enerji oranı

Özet: Enerjiye dayalı sismik tasarımda deprem yer hareketi yapılara enerji girişi olarak dikkate alınmaktadır. Sisteme giren enerji kinetik enerji, sönüm enerjisi, elastik şekil değiştirme enerjisi ve histeretik enerji şeklindeki bileşenlerin toplamı olup histeretik enerji doğrudan yapısal hasar ile ilişkilidir. Literatürde histeretik enerjinin belirlenmesine yönelik histeretik modeli, sönüm oranını ve sünekliği esas alan çok sayıda ampirik bağıntı vardır. Buna karşın bu bağıntılar yer hareketinin özelliklerini dikkate almamaktadır. Bu çalışmada, enerjilerin hesabı için zaman tanım alanında doğrusal elastik olmayan analiz kullanılmış ve tek serbestlik dereceli (TSD) sisteme giren deprem enerjisi ile histeretik enerjinin yer hareketi süresi boyunca değişimi incelenmiştir. Dinamik analizlerde aynı zeminler üzerinde kaydedilmiş yedi adet yer hareketi ve farklı süneklik oranları ve doğal periyotları bulunan üç adet bilineer TSD sistem kullanılmıştır. Doğrusal olmayan dinamik analizlerin sonucunda birim kütle başına enerji girişi ve histeretik enerji grafiksel olarak elde edilmiştir. Histeretik enerji/toplam enerji oranı (E_H/E_I) ile diğer enerji bileşenlerinin giren enerjiye oranı araştırılmıştır. Doğrusal olmayan dinamik analizlerden elde edilen E_H/E_I oranları ile ampirik yaklaşımlara ait oranlarla karşılaştırılmış ve tutarlı sonuçlar elde edilmiştir. Ortalama E_H/E_I oranı 0.468 ile 0.488 arasında değişmektedir ki bu da toplam enerji girdisinin yarısına yakın kısmının doğrusal olmayan davranış yoluyla tüketildiğini göstermektedir.

1. Introduction

Conventional design and analysis methods mainly focus on establishing a particular peak demand parameter such as member force, maximum displacement and displacement ductility. In these design procedures, capacity of structural components is taken to be independent of the earthquake excitation and the cumulative damage associated with ground motion duration and numerous inelastic deformation cycles that the structure might experiences is not accounted for. Although displacement-based seismic design methods correlating the imposed displacement to the structure and the structural damage have recently been developed, the problem related to the cumulative damage has not been overcome. Accordingly, neither force-based methods nor displacement-based methods provide the whole necessary information to quantify the level of structural damage.

More recently, it has been widely recognized that the energy is one of the key factors related to the structural damage in strong ground motions since the level of damage depends on both maximum deformations and response history characteristics. Accordingly, more rational seismic design methods based on energy criteria incorporating forces and displacements have been developed where the loading effect of earthquake is interpreted in terms of input energy (E_I) [1–14]. These pioneer studies have provided new insights into the field of modern earthquake engineering and the energy concept is an important topic of current interest [15–27]. Since the earthquake input energy is estimated as the integral of velocity response of inelastic system with respect to earthquake duration, all of the inelastic deformation cycles are considered in energy-based methods. Another major advantage of energy-based approach is that the structural resistance and the earthquake effect in terms of energy are basically uncoupled since input energy is a quite stable response parameter and hardly depends on hysteretic characteristics of the structure. Accordingly, there have been extensive attempts for estimating earthquake input energy [28–42].

Usually, the design criterion in energy-based methods is satisfied by providing adequate capacity to dissipate the seismic energy imposed on structures by earthquake ground motions. Therefore, in order to achieve energy-based design criteria, it seems quite imperative to have the accurate evaluation of both seismic energy demands and energy dissipation capacity of structural components which strongly depends on the loading history. Meanwhile, quantification of the demand in terms of energy is the preliminary task. When the structure comes to rest at the end of the ground motion, the kinetic energy (E_K) and the elastic strain energy (E_S) of the system

essentially vanishes and the total energy imposed by the earthquake excitation is dissipated in part by the damping energy (E_D) and the hysteretic energy (E_H) components. Meanwhile, estimation of hysteretic energy demands imparted to structures by earthquake ground motion is a crucial issue since it is associated with the damage potential of structures. In this regard accurate estimation of the portion of cumulative hysteretic energy to energy input is of great importance. Moreover, it would be quite easy to compute the hysteretic energy demand from input energy spectra if the ratio of hysteretic energy to energy input was known. Accordingly, several approximations have been proposed in order to estimate hysteretic energy demand and the hysteretic energy to input energy ratio (E_H/E_I) in structures [43–57].

The main objective of the paper is to obtain input and hysteretic energy time history curves of several inelastic SDOF systems by means of NLTH analysis and to investigate the effectiveness of some approximate methods related to hysteretic and input energy. Accordingly, three SDOF systems having natural periods as 0.2 s, 0.6 s and 1.0 s are selected to perform energy analyses. Firstly, the hysteretic energy to energy input ratio versus time (E_H/E_I-t) graphs of bilinear SDOF systems with a damping ratio of 5% and a ductility ratio of 2 are obtained from NLTH analyses. Subsequently, E_H/E_I ratios obtained from reference approximations are indicated in these graphs with the result graphs of nonlinear dynamic analyses. Finally, E_H/E_I ratios from time history analyses are compared with E_H/E_I values of approximate estimations. The results and findings of the study are presented by graphs and tables.

2. Seismic Energy Components

The general energy balance of structural systems can be derived by integrating the governing equation of motion with respect to relative displacement of the mass. Energy components which are defined in energy-based seismic design and evaluation rise from the integral terms of this equation. Consequently, the energy balance equation of an SDOF system can be written as in the form of its well-known expression from dynamics of structures as given in Eq. (1) [2, 4, 5, 13, 15, 21, 25, 26, 32, 37, 40, 41, 46].

$$\int_0^u m \ddot{u}(t) du + \int_0^u c \dot{u}(t) du + \int_0^u f_s du = - \int_0^u m \ddot{u}_g(t) du \quad (1)$$

In the basic energy balance equation; m is the seismic mass of the structure, c is the damping coefficient, u is the relative displacement of the system, f_s is the restoring force, $\ddot{u}_g(t)$ is the horizontal ground

acceleration, $\dot{u}(t)$ is the relative velocity and $\ddot{u}(t)$ is the relative acceleration of the system. The right-hand side of Eq. (1) expresses the total energy input to the system (E_I) with the strong ground acceleration. The energy input (E_I) points out the energy demand of an earthquake and imposes the seismic energy to the structure. The first term on the left-hand side of Eq. (1) represents the kinetic energy of the mass (E_K), the second term represents the damping energy (E_D) and the last term indicates the total absorbed energy by the structure with both linear-elastic and nonlinear behavior (E_a). The summation of these energy components constitutes the total energy input and Eq. (1) can be rewritten by using the symbolic seismic energy terms as:

$$E_K + E_D + E_a = E_I \quad (2)$$

The absorbed energy (E_a) term also includes both the elastic strain energy component (E_S) and the hysteretic energy component (E_H). Hysteretic energy is generally considered to be the most important energy component contributing to structural damage [13, 21, 46, 56]. It may be thought that the hysteretic energy composing the very significant portion of the absorbed energy is directly related with inelastic response of the system. Besides Eq. (2) can be rewritten by expanding the total absorbed energy (E_a) in terms of the elastic strain energy (E_S) and the hysteretic energy (E_H) as:

$$E_K + E_D + \{E_S + E_H\} = E_I \quad (3)$$

Eq. (3) yields the energy response parameters of SDOF systems subjected to earthquake excitation. E_S has the significant portion in the elastic response of the system whereas it approaches nearly to zero at the end of the ground motion. In inelastic behavior of the system, the components E_K and E_S are negligible compared to E_H and almost at the end of the earthquake ground motion, Eq. (3) may be practically expressed as:

$$E_D + E_H \cong E_I \quad (4)$$

3. Reference Approximations for Hysteretic to Input Energy Ratio

In scientific literature there exist many previous studies related to the hysteretic energy to input energy ratio (E_H/E_I) of SDOF systems. Researchers generally defined E_H/E_I ratio as functions of viscous damping ratio (ξ), ductility factor (μ) and the hysteretic behavior [2, 3, 43, 44, 56, 57]. Akiyama proposed a relationship between the input and hysteretic energies in terms of equivalent velocities [3]. Based on analysis of SDOF systems having elastic-perfectly plastic restoring force characteristics, Akiyama expressed the ratio of damage velocity (as a function of the energy contributing to damage) to the equivalent velocity (as a function of E_I) in terms of the

viscous damping ratio (ξ). At the end of the earthquake ground motion duration since E_K and E_S components are almost zero, the energy which contributes to structural damage can be approximately taken equal to the hysteretic energy E_H [40]. Accordingly, Akiyama's empirical expression is given below [3]:

$$\frac{E_H}{E_I} \cong \frac{1}{(1 + 3 \cdot \xi + 1.2 \cdot \sqrt{\xi})^2} \quad (5)$$

Fajfar and Vidic [43] proposed an expression based on the results of some parametric studies considering elastic-perfectly plastic SDOF systems. They expressed E_H/E_I ratio as a function of viscous damping (ξ), ductility factor (μ) and hysteretic behavior [43, 56]. Their simple formula to describe E_H/E_I ratio is as follows:

$$\frac{E_H}{E_I} = c_E \cdot \frac{(\mu - 1)^{c_H}}{\mu} \quad (6)$$

where c_E and c_H coefficients depending on the type of hysteretic model and damping model are taken to be 1.05 and 0.95 for 5% damping, respectively [43]. These coefficients used within the study are for bilinear hysteretic model and instantaneous-stiffness-proportional damping.

Manfredi [44] used many earthquake acceleration records and carried out statistical analyses on the used ground motion records. The following expression was given by Manfredi for the damping ratio equal to 0.05:

$$\frac{E_H}{E_I} = 0.72 \cdot \frac{(\mu_c - 1)}{\mu_c} \quad (7)$$

where μ_c is the cyclic ductility ratio [44].

Khashae [57] eliminated the cyclic ductility μ_c in Manfredi's formula and applied regression analysis on hysteretic and input energy data obtained from 160 accelerograms and proposed an expression for E_H/E_I ratio for systems having $\mu=2, 3, 4$ and 5 as:

$$\frac{E_H}{E_I} = 0.72 \cdot \left(1 - \frac{1}{\mu}\right)^{0.7} \quad (8)$$

In addition to the above empirical formulas, an extensive research has been devoted to estimate the ratio of E_H/E_I . Kuwamura and Galambos [4], Akbaş et al. [15], Decanini and Mollaioli [16] and Benavent et al. [32, 37] are some of the leading researchers who made studies to estimate the ratio of E_H/E_I in SDOF systems [40]. It was clearly seen from these researchers' studies that proposed expressions to estimate the ratio of E_H/E_I are overly conservative and generally overestimate the E_H/E_I ratio [25].

Table 1. Major seismological parameters of the assembled ground motions

Record Name	Earthquake & Year	Station	M_w	R_{JB} (km)	V_{S30} (m/s)	PGA (g)	PGV (cm/s)	PGD (cm)
BIGBEAR_HOS180	Big Bear-01, 1992	San Bernardino-E & Hospitality	6.46	34.98	296.97	0.101	11.85	3.36
BORREGO_A-ELC180	Borrego Mtn, 1968	El Centro Array #9	6.63	45.12	213.44	0.133	26.71	14.56
ERZINCAN_ERZ-EW	Erzincan, Turkey, 1992	Erzincan	6.69	0.0	352.05	0.496	78.16	28.04
KOCAELI_DZC180	Kocaeli, Turkey, 1999	Duzce	7.51	13.60	281.86	0.312	58.85	44.05
LANDERS_YER360	Landers, 1992	Yermo Fire Station	7.28	23.62	353.63	0.152	29.60	24.83
MANAGUA_A-ESO180	Managua, Nikaragua-01, 1972	Managua, ESSO	6.24	3.51	288.77	0.330	30.76	6.20
TRINIDAD.B_B-RDL270	Trinidad, 1980	Rio Dell Overpass-FF	7.20	76.06	311.75	0.151	8.88	3.63

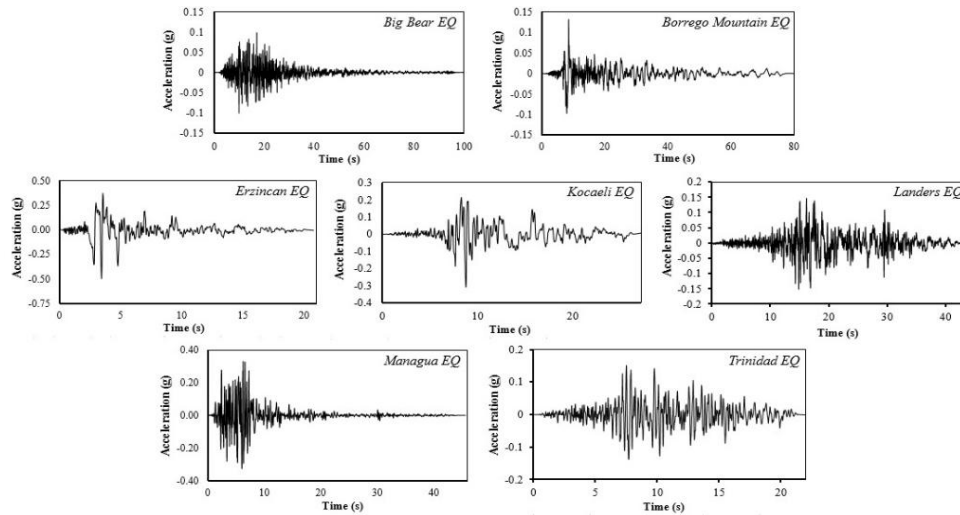


Figure 1. Acceleration time histories of the assembled ground motions

In the presented study, both the input energy and hysteretic energy demands of SDOF structures and E_H/E_I ratios are obtained by means of NLTH analysis using the assembled ground motions and the results of E_H/E_I ratios are compared with those of Eqs. (5)-(8).

4. Ground Motion Database

A total of seven real accelerograms are assembled considering the magnitude, distance, fault type, and soil profile type information. The accelerograms are compiled from the strong ground motion database of Pacific Earthquake Engineering Research Center [58]. The accelerograms have a magnitude range of 6.5 to 7.5 and a source-to-site distances less than 80 km. The peak ground acceleration (PGA) value of the earthquake ground motions is larger than 0.1g, where g is the gravitational acceleration. The site conditions of the assembled accelerograms represent the features of NEHRP site class D (stiff soil) according the available average shear-wave velocity to 30 m depth of subsoil (V_{S30}). The selected ground motions have strike-slip focal mechanism. It should also be noted that the selected ground motion records are identified as no pulse-like records in the Pacific Earthquake Engineering Research Center (PEER) ground motion database. The overall characteristics of the collected strong ground motion

records are presented in Table 1, where M_w is the moment magnitude of earthquake, R_{JB} is the Joyner-Boore distance, PGV and PGD are the peak values of ground velocity and ground displacement, respectively. Meanwhile, the acceleration time histories of the assembled ground motions are demonstrated in Fig. 1.

Horizontal components of actual accelerograms are considered in NLTH analysis for energy calculations and the structural response to one horizontal component is evaluated. The action effects due to the combination of the horizontal components of ground motion is not taken into consideration in order to obtain input (E_I) and hysteretic (E_H) energy time history curves, as well as E_H/E_I variations.

Plotted in Fig. 2 is the non-scaled inelastic acceleration response spectra of individual records developed for a damping ratio of 5%. Response spectra are constructed using PRISM software [59]. The ground motion records are not scaled since the paper does not focus on estimating of input and hysteretic energy time history curves of inelastic SDOF systems subjected to earthquake ground motions compatible with elastic design acceleration spectra of any earthquake design code. The study only evaluates E_H/E_I ratios the selected SDOF systems under a set of non-scaled recorded earthquake under ground motions.

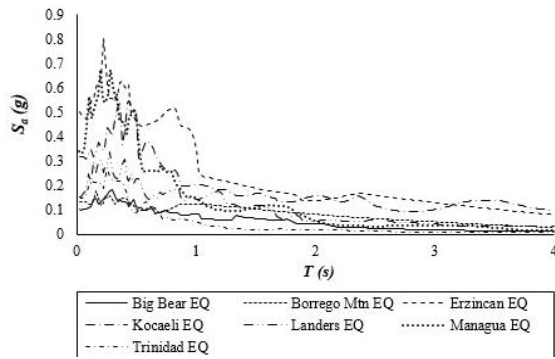


Figure 2. Inelastic acceleration spectra of the records

5. Characteristics of SDOF Systems and Energy Graphs

Three SDOF systems having various natural periods of $T_n=0.2$ s, 0.6 s and 1.0 s are selected as shown in Fig. 3. A constant ductility demand of $\mu=2$ is taken into consideration. Pre-yield damping ratio is taken as $\xi=5\%$.

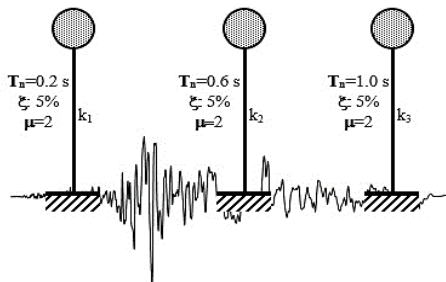


Figure 3. SDOF systems having different natural periods with $\mu=2$

The non-linear material behavior is modeled as a bilinear non-degrading hysteretic model with post-yield strain-hardening ratio of 10% (Fig. 4). Strength degradation and pinching effects are neglected within the study. Many structures subjected to reverse cyclic loading exhibit some level of stiffness and strength degradation [59]. However, the implemented hysteretic model does not incorporate any level of strength or stiffness degradation. The motivation of a simpler bilinear hysteretic model relies on the fact that the approximate formulas considered in the study are mainly based on elasto-plastic (a bilinear strength hardening model with post-yield stiffness equal to zero) or bilinear non-degrading hysteretic model.

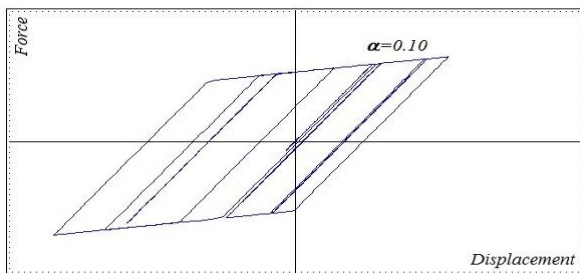


Figure 4. Bilinear non-degrading hysteretic model with 10% strain hardening

Both the input energy and hysteretic energy graphs of SDOF systems in Fig. 3 are obtained by using the relevant expressions in Eq. (1). Earthquake input energies are computed from the right-hand side of general energy balance equation and hysteretic energies are determined from the last term (inelastic part) of the left-hand side of the same equation. Velocity time histories of inelastic SDOF systems subjected to horizontal component of earthquake ground motions in Fig. 1 are computed by using PRISM Software [60]. Then, hysteretic energies and input energies are computed by using the Excel programming written by the authors.

Fig. 5 is a representative figure which explains the graphs of input and hysteretic energy time histories. Hysteretic energy tends to be constant over very large duration of earthquake ground motion and is considered to be the main design parameter in energy based seismic design of structures [15, 25]. Nonetheless, hysteretic to input energy (E_H/E_I) ratio generally tends to be constant over the certain duration of ground motion.

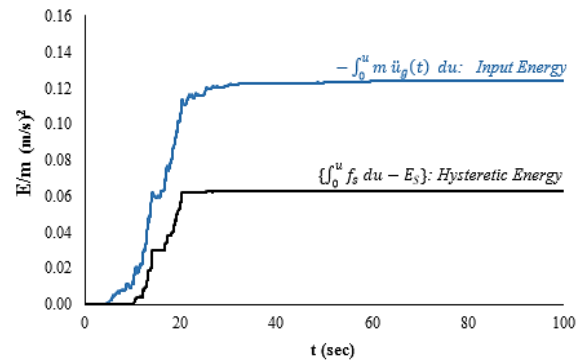


Figure 5. Input and hysteretic energy graphs of an SDOF system under an earthquake effect

6. Hysteretic to Input Energy Ratios of SDOF Systems

Nonlinear response parameters (i.e. nonlinear displacements and velocities) of the SDOF systems subjected to assembled ground motions are obtained through NLTH analysis. Firstly, seismic energy input to the systems is determined by integrating the product of ground motion accelerations and nonlinear velocities over the entire duration of the earthquake. In this way time histories of seismic input energy per unit mass are assessed. Then, hysteretic energy demands for SDOF systems are obtained by integrating the resulting nonlinear forces of dynamic analysis over the earthquake duration. It is quite significant to estimate the hysteretic energy demand since in energy based design procedures the structural damage is limited by providing adequate dissipated energy capacity of the structural system. Accordingly, shown in Fig. 6 are the input and hysteretic energy time histories of inelastic SDOF systems subjected to assembled ground motions.

Fig. 6 indicates that the maximum input and hysteretic energies occur at the end of the earthquake excitation. Therefore, the duration of earthquake ground motion affects these energy components. The dissipated hysteretic energy increases as SDOF systems experience inelastic deformations. However, it is almost zero at the linear elastic response of the systems. Similarly, elastic input energy is very small. The maximum E_i/m values obtained for the considered SDOF systems are listed in Table 2.

Table 2. Maximum input energy per unit mass

Earthquake	$E_{i,max}/m$ (m^2/s^2)		
	$(\mu=2, \xi=5\%, \alpha=0.10)$		
	$T=0.2$ s	$T=0.6$ s	$T=1.0$ s
Big Bear EQ	0.0311	0.1242	0.0958
Borrogo Mtn EQ	0.0123	0.0674	0.1195
Erzincan EQ	0.3134	0.9215	0.7886
Kocaeli EQ	0.0494	0.3971	0.4970
Landers EQ	0.0718	0.1603	0.2621
Managua EQ	0.2251	0.5962	0.2855
Trinidad EQ	0.0461	0.0712	0.0501

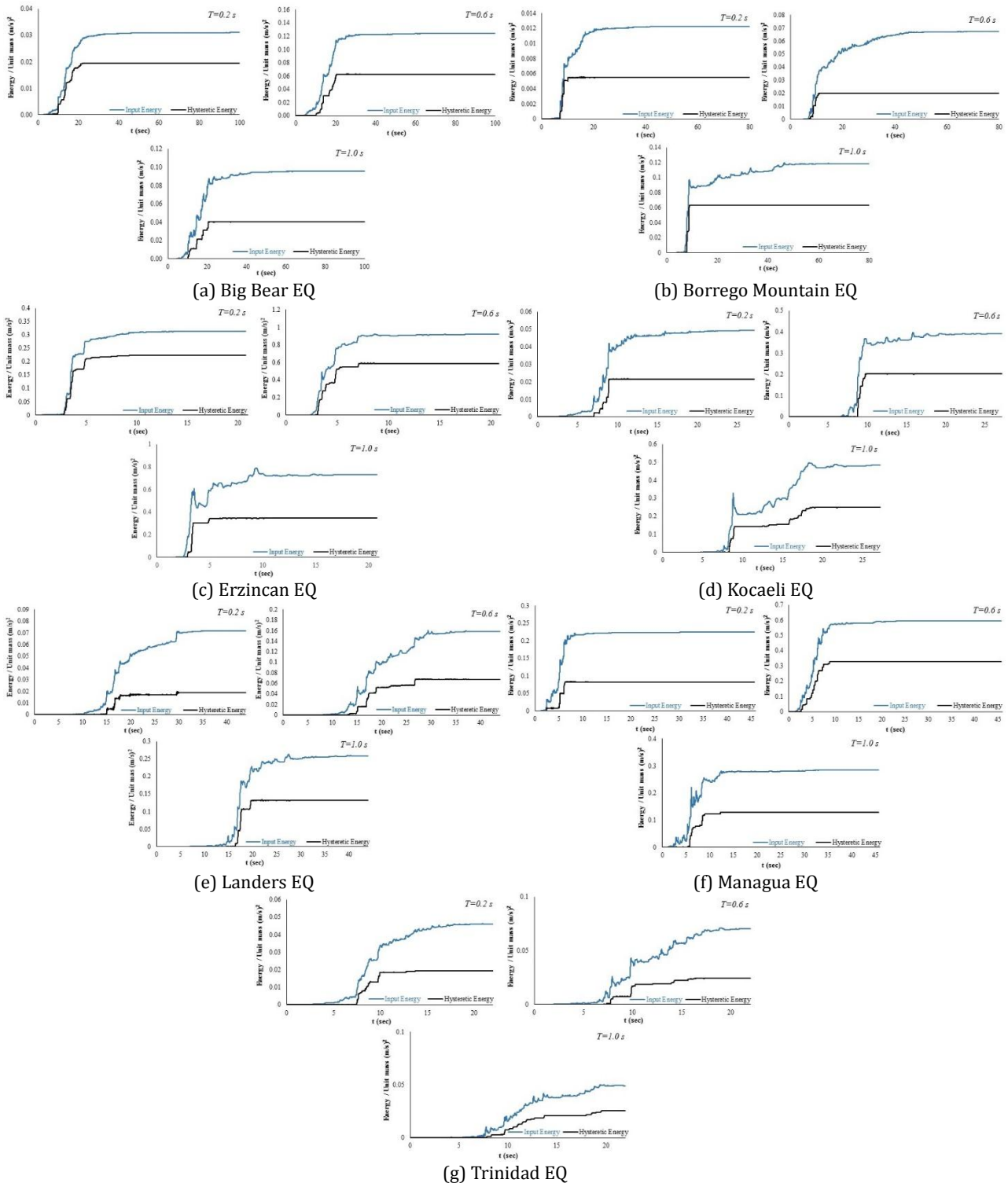


Figure 6. Input and hysteretic energy time histories of SDOF systems with $\mu=2$, $\alpha=0.10$ and $\xi=5\%$

After estimating the seismic energy demand imposed by the earthquake, the percentage of the input energy to be dissipated through inelastic hysteretic behavior is calculated and the variation of hysteretic energy to input energy (E_H/E_I) ratio is obtained (Fig. 7). The results of the time history analyses show that this ratio is a stable quantity. Additionally, the constant E_H/E_I ratios obtained from the reference empirical approximations are also plotted in Fig. 7. Approximate E_H/E_I ratios are quite close to each other and it is found that the reference approximate

formulas estimate E_H/E_I ratios within reasonable limits.

Table 3 summarizes the maximum E_H/E_I ratios of the individual ground motions as well as the approximate estimations of different researchers. It is observed that the average of E_H/E_I ratios is rather constant and the reference empirical formulas estimate this value quite reasonable rather than the E_H/E_I ratios of individual earthquakes.

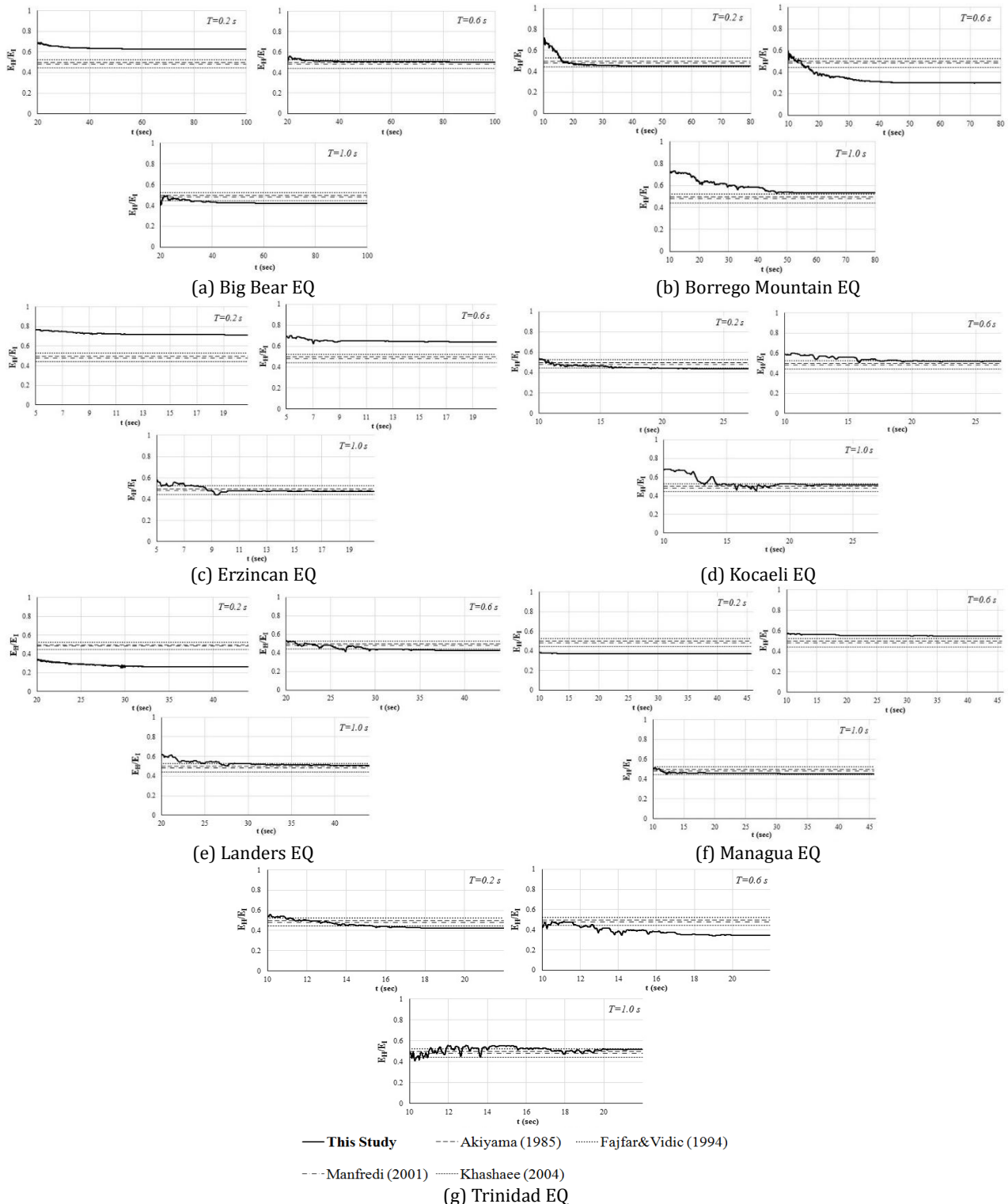


Figure 7. E_H/E_I variation of SDOF systems with $\mu=2$, $\alpha=0.10$ and $\xi=5\%$

Table 3. E_H/E_I ratios at the end of the duration of earthquakes ($\mu=2$, $\alpha=0.10$, $\xi=5\%$)

E_H/E_I	<i>This Study</i> ($T=0.2$ s)	<i>This Study</i> ($T=0.6$ s)	<i>This Study</i> ($T=1.0$ s)	<i>Akiyama</i> (1985)	<i>Fajfar&Vidic</i> (1994)	<i>Manfredi</i> (2001)	<i>Khashaee</i> (2004)
Big Bear EQ	0.627	0.504	0.419				
Borrego Mtn EQ	0.449	0.297	0.533				
Erzincan EQ	0.715	0.640	0.472				
Kocaeli EQ	0.436	0.517	0.512	0.497	0.525	0.480	0.443
Landers EQ	0.261	0.427	0.511				
Managua EQ	0.368	0.550	0.451				
Trinidad EQ	0.421	0.344	0.516				
MEAN	0.468	0.468	0.488			0.486	

Table 4. Energy ratios of bilinear SDOF systems near the end of the earthquake duration

Earthquake	$E_{K+E_D+E_S}$ (%)			E_H (%)		
	$T=0.2$ s	$T=0.6$ s	$T=1.0$ s	$T=0.2$ s	$T=0.6$ s	$T=1.0$ s
Big Bear EQ	37.31	49.61	58.09	62.69	50.39	41.91
Borrego Mtn EQ	55.10	70.35	46.70	44.90	29.65	53.30
Erzincan EQ	28.53	36.09	52.82	71.47	63.91	47.18
Kocaeli EQ	56.42	48.29	48.80	43.58	51.71	51.20
Landers EQ	73.90	57.30	48.90	26.10	42.70	51.10
Managua EQ	63.20	44.99	54.90	36.80	55.01	45.10
Trinidad EQ	57.90	65.58	48.40	42.10	34.42	51.60

The portion of the earthquake input energy distributed among the total of the kinetic energy of the mass, the damping energy and the elastic strain energy ($E_K+E_D+E_S$) and the hysteretic energy (E_H) is listed in Table 4 in percent. For all period values, the summation of these values corresponds to the total of the input energy (E_I). All earthquake ground motions reflect their own characteristics to results. It should also be noted that more realistic results may be calculated using ground motion records containing accelerograms of two horizontal components. However, considering the limits of the software used for seismic response analysis of SDOF systems in the study, the seismic action is described by one horizontal component. This point should be taken into consideration in order to evaluate the results of the input and hysteretic energy computations of this study.

7. Conclusions and Recommendations

Earthquake input energy can be used as a measure of the intensity of ground motion and besides it accounts for the duration of ground motion. Having estimated the energy input to the system (e.g. from energy input spectrum), one can easily determine the portion of the input energy converted to hysteretic energy since E_H/E_I is generally supposed to be a stable quantity. In this study, input and hysteretic energy time histories of SDOF structures having bilinear behavior under the effect of selected earthquakes are investigated. E_H/E_I ratio graphs are obtained from nonlinear time history analyses and compared with some approximate formulas given by prior researchers.

Earlier studies indicated that structural properties such as ductility, damping ratio and the shape of hysteresis loop do have a significant influence on

earthquake input energy and hysteretic energy time histories of structures. It is found that the characteristics of the employed earthquake ground motions significantly affect the energy time histories. Maximum input energies have tendency to increase from $T_n=0.2$ s to $T_n=0.6$ s for almost all selected earthquakes while there is an increasing or decreasing in the energies from $T_n=0.6$ s to $T_n=1.0$ s. Erzincan Earthquake gives the maximum input and hysteretic energies among all selected earthquakes, for SDOF systems having $\mu=2$, $\xi=5\%$ and $\alpha=0.10$. Considering the results of the presented study, it can be concluded that the input energy and especially the hysteretic energy tend to be constant over a wide duration range. In respect to this, E_H/E_I ratios are generally obtained almost constant at the same duration range. Nonlinear time history results are compared to the approximate results given in Eqs. (5)-(8). Fajfar and Vidic's estimation about E_H/E_I ratio gives the maximum value as 0.525, the second maximum is Akiyama's approximation as 0.497, then Manfredi's formula gives $E_H/E_I=0.480$ and finally the value of 0.443 is obtained from Khashaee's equation as the minimum among all considered estimations in the study. Time history results for E_H/E_I ratios give very compatible results with selected researchers' approximate estimations. For E_H/E_I ratios; the mean result of time history analyses for $T_n=0.2$ s and $T_n=0.6$ s is obtained as 0.468 and the mean result for $T_n=1.0$ s is obtained as 0.488. The mean value of selected researchers' formulas is calculated as 0.486. The mean results of E_H/E_I ratios are obtained too close within this study when the results of time history analyses and approximate equations are compared.

Further research may be conducted to obtain more detailed conclusion about the dissipation of hysteretic energy in SDOF systems and the variation of E_H/E_I ratios. More ground motion records can be

used to generalize the energy results. Using a wide range of ground motion set may lead to more sensitive and more reliable generalizations about the E_H/E_I ratios. Analyses may be performed to determine the input energy and hysteretic energy dissipation of multi-degree-of-freedom (MDOF) systems. Moreover, different hysteretic models, ductility ratios, damping ratios and characteristics of earthquake ground motion records used in the analyses can change the energy results. The other researchers' estimations may be investigated to compare the degree of approximation of E_H/E_I ratios with the results of dynamic analyses.

In this study, ground motion records are selected based on magnitude, distance, and focal mechanism and it is only aimed to obtain E_H/E_I ratios from time history analyses and from approximate formulas. If seismic assessment is to be performed, the rigorous selection of ground motions will be an important consideration and holistic ground motion selection methods should be used for realistic structural responses.

References

- [1] Housner, G.W. 1956. Limit Design of Structures to Resist Earthquakes. Proceedings of the 1st World Conference on Earthquake Engineering, Berkeley, CA, 186-198.
- [2] Zahrah, T.F., Hall, W.J. 1984. Earthquake Energy Absorption in SDOF Structures. Journal of Structural Engineering, 110(8), 1757-1772.
- [3] Akiyama, H. 1985. Earthquake Resistant Limit State Design for Buildings. University of Tokyo Press, Japan.
- [4] Kuwamura, H., Galambos, T.V. 1988. Earthquake Load for Structural Reliability. Journal of Structural Engineering, 115(6), 1446-1462.
- [5] Uang, C.M., Bertero, V.V. 1990. Evaluation of Seismic Energy in Structures. Earthquake Engineering & Structural Dynamics, 19(1), 77-90.
- [6] Fajfar, P. 1992. Equivalent Ductility Factors, Taking into Account Low-Cycle Fatigue. Earthquake Engineering & Structural Dynamics, 21(10), 837-848.
- [7] Rodriguez, M. 1994. A Measure of the Capacity of Earthquake Ground Motions to Damage Structures. Earthquake Engineering & Structural Dynamics, 23(6), 627-643.
- [8] Chai, Y.H., Fajfar, P., Romstad, K.M. 1998. Formulation of Duration-Dependent Inelastic Seismic Design Spectrum. Journal of Structural Engineering, 124(8), 913-921.
- [9] Tso, W.K., Zhu, T.J., Heidebrecht, A.C. 1993. Seismic Energy Demands on Reinforced Concrete Moment-Resisting Frames. Earthquake Engineering & Structural Dynamics, 22(6), 533-545.
- [10] Sucuoğlu, H., Nurtuğ, A. 1995. Earthquake Ground Motion Characteristics and Seismic Energy Dissipation. Earthquake Engineering & Structural Dynamics, 24(9), 1195-1213.
- [11] Nakashima, M., Saburi, K., Tsuji, B. 1996. Energy Input and Dissipation Behaviour of Structures with Hysteretic Dampers. Earthquake Engineering & Structural Dynamics, 25(5), 483-496.
- [12] Goel, R.K. 1997. Seismic Response of Asymmetric Systems: Energy-Based Approach. Journal of Structural Engineering, 123(11), 1444-1453.
- [13] Shen, J., Akbaş, B. 1999. Seismic Energy Demand in Steel Moment Frames. Journal of Earthquake Engineering, 3(04), 519-559.
- [14] Ye, L., Otani, S. 1999. Maximum Seismic Displacement of Inelastic Systems Based on Energy Concept. Earthquake Engineering & Structural Dynamics 28(12), 1483-1499.
- [15] Akbas, B., Shen, J., Hao, H. 2001. Energy Approach in Performance-Based Seismic Design of Steel Moment Resisting Frames for Basic Safety Objective. The Structural Design of Tall Buildings, 10(3), 193-217.
- [16] Decanini, L. D., Mollaioli, F. 2001. An Energy-Based Methodology for the Assessment of Seismic Demand. Soil Dynamics and Earthquake Engineering, 21(2), 113-137.
- [17] Wong, K.K.F., Yang, R. 2002. Earthquake Response and Energy Evaluation of Inelastic Structures. Journal of Engineering Mechanics, 128(3), 308-317.
- [18] Chou, C.C., Uang, C.M. 2003. A Procedure for Evaluating Seismic Energy Demand of Framed Structures. Earthquake Engineering & Structural Dynamics, 32(2), 229-244.
- [19] Wong, K.K. 2004. Inelastic Seismic Response Analysis Based on Energy Density Spectra. Journal of Earthquake Engineering, 8(2), 315-334.
- [20] Chai, Y.H. 2005. Incorporating Low-Cycle Fatigue Model into Duration-Dependent Inelastic Design Spectra. Earthquake Engineering & Structural Dynamics, 34(1), 83-96.
- [21] Kalkan, E., Kunnath, S.K. 2008. Relevance of Absolute and Relative Energy Content in Seismic Evaluation of Structures. Advances in Structural Engineering, 11(1), 17-34.
- [22] Lei, C., Xianguo Y., Kangning L. 2008. Analysis of Seismic Energy Response and Distribution of RC Frame Structures. Proceedings of the 14th

- World Conference on Earthquake Engineering, October 12-17, Beijing, China.
- [23] Ye, L., Cheng, G., Qu, Z. 2009. Study on Energy-Based Seismic Design Method and Application on Steel Braced Frame Structures. Proceedings of the 6th International Conference on Urban Earthquake Engineering, March 3-4, Tokyo Institute of Technology, Tokyo, Japan, 417-428.
- [24] Kazantzi, A.K., Vamvatsikos, D. 2012. A Study on the Correlation Between Dissipated Hysteretic Energy and Seismic Performance. Proceedings of the 15th World Conference on Earthquake Engineering, September 24-28, Lisbon, Portugal.
- [25] Mezgebo, M.G. 2015. Estimation of earthquake input energy, hysteretic energy and its distribution in MDOF structures. Syracuse University, PhD Dissertation, 274 p, Syracuse, New York.
- [26] Dogru, S., Aksar, B., Akbas, B., Shen, J., Seker, O., Wen, R. 2016. Seismic Energy Demands in Steel Moment Frames. Applied Mechanics and Materials, 847, 210-221.
- [27] Donaire-Ávila, J., Benavent-Climent, A., Lucchini, A., Mollaioli, F. 2017. Energy-Based Seismic Design Methodology: A Preliminary Approach. Proceedings of the 16th World Conference on Earthquake Engineering, January 9-13, Santiago Chile, Paper No. 2106.
- [28] Fajfar, P., Vidic, T., Fischinger, M. 1989. Seismic Design in Medium- and Long Period Structures. Earthquake Engineering & Structural Dynamics, 18(8), 1133-1144.
- [29] Kuwamura, H., Kirino, Y., Akiyama, H. 1994. Prediction of Earthquake Energy Input from Smoothed Fourier Amplitude Spectrum. Earthquake Engineering & Structural Dynamics, 23(10), 1125-1137.
- [30] Decanini, L.D., Mollaioli, F. 1998. Formulation of Elastic Earthquake Input Energy Spectra. Earthquake Engineering & Structural Dynamics, 27(12), 1503-1522.
- [31] Chou, C.C., Uang, C.M. 2000. Establishing Absorbed Energy Spectra - An Attenuation Approach. Earthquake Engineering & Structural Dynamics, 29(10), 1441-1455.
- [32] Benavent-Climent, A., Pujades, L.G., López-Almansa, F. 2002. Design Energy Input Spectra for Moderate-Seismicity Regions. Earthquake Engineering & Structural Dynamics, 31(5), 1151-1172.
- [33] Kalkan, E., Kunnath, S.K. 2007. Effective Cyclic Energy as a Measure of Seismic Demand. Journal of Earthquake Engineering, 11(5), 725-751.
- [34] Teran-Gilmore, A., Jirsa, J.O. 2007. Energy Demands for Seismic Design Against Low-Cycle Fatigue. Earthquake Engineering & Structural Dynamics, 36(3), 383-404.
- [35] Amiri, G.G., Darzi, G.A., Amiri, J.V. 2008. Design Elastic Input Energy Spectra Based on Iranian Earthquakes. Canadian Journal of Civil Engineering, 35(6), 635-646.
- [36] Teran-Gilmore, A., Bahena-Arredondo, N. 2008. Cumulative Ductility Spectra for Seismic Design of Ductile Structures Subjected to Long Duration Motions: Concept and Theoretical Background. Journal of Earthquake Engineering, 12(1), 152-172.
- [37] Benavent-Climent, A., López-Almansa, F., Bravo-González, D.A. 2010. Design Energy Input Spectra for Moderate-to-High Seismicity Regions Based on Colombian Earthquakes. Soil Dynamics and Earthquake Engineering, 30(11), 1129-1148.
- [38] Tselentis, G.A., Danciu, L., Sokos, E. 2010. Probabilistic Seismic Hazard Assessment in Greece - Part 2: Acceleration Response Spectra and Elastic Input Energy Spectra. Natural Hazards and Earth System Sciences, 10(1), 41-49.
- [39] Okur, A., Erberik, M.A. 2012. Adaptation of Energy Principles in Seismic Design of Turkish RC Frame Structures. Part I: Input Energy Spectrum. Proceedings of the 15th World Conference on Earthquake Engineering, September 24-28, Lisbon, Portugal.
- [40] Lopez-Almansa, F., Yazgan, A.U., Benavent-Climent, A. 2013. Design Energy Input Spectra for High Seismicity Regions Based on Turkish Registers. Bulletin of Earthquake Engineering, 11(4), 885-912.
- [41] Dindar, A.A., Yalçın, C., Yüksel, E., Özkaynak, H., Büyüköztürk, O. 2015. Development of Earthquake Energy Demand Spectra. Earthquake Spectra, 31(3), 1667-1689.
- [42] Alıcı, F.S., Sucuoğlu, H. 2016. Prediction of Input Energy Spectrum: Attenuation Models and Velocity Spectrum Scaling. Earthquake Engineering & Structural Dynamics, (45)13, 2137-2161.
- [43] Fajfar, P., Vidic, T. 1994. Consistent Inelastic Design Spectra: Hysteretic and Input Energy. Earthquake Engineering & Structural Dynamics, 23(5), 523-537.
- [44] Manfredi, G. 2001. Evaluation of Seismic Energy Demand. Earthquake Engineering & Structural Dynamics, 30(4), 485-499.
- [45] Riddell, R., Garcia, J.E. 2001. Hysteretic Energy Spectrum and Damage Control. Earthquake Engineering & Structural Dynamics, 30(12), 1791-1816.

- [46] Khashaei, P., Mohraz, B., Sadek, F., Lew, H.S. Gross, J.L. 2003. Distribution of Earthquake Input Energy in Structures. NISTIR 6903, Building and Fire Research Laboratory, National Institute of Standards and Technology, Gaithersburg.
- [47] Estes, K.R., Anderson, J.C. 2004. Earthquake Resistant Design Using Hysteretic Energy Demands for Low Rise Buildings. Proceedings of the 13th World Conference on Earthquake Engineering, August 1-6, Vancouver, Canada, Paper No. 3276.
- [48] Sawada, K., Matsuo, A., Ujiie, K. 2005. A Study on Hysteretic Plastic Energy Input into Single and Multi Degree of Freedom Systems Subjected to Earthquakes. WIT Transactions on The Built Environment, 81, 269-280.
- [49] Arroyo, D., Ordaz, M. 2007. Hysteretic Energy Demands for SDOF Systems Subjected to Narrow Band Earthquake Ground Motions. Applications to the Lake Bed Zone of Mexico City. Journal of Earthquake Engineering, 11(2), 147-165.
- [50] Arroyo, D., Ordaz, M. 2007. On the Estimation of Hysteretic Energy Demands for SDOF Systems. Earthquake Engineering & Structural Dynamics, 36(15), 2365-2382.
- [51] Prasanth, T., Ghosh, S., Collins, K.R. 2008. Estimation of Hysteretic Energy Demand Using Concepts of Modal Pushover Analysis. Earthquake Engineering & Structural Dynamics, 37(6), 975-990.
- [52] Bojorquez, E., Teran-Gilmore, A., Ruiz, S.E., Reyes-Salazar, A. 2011. Evaluation of Structural Reliability of Steel Frames: Interstory Drift Versus Plastic Hysteretic Energy. Earthquake Spectra, 27(3), 661-682.
- [53] Wang, F., Yi, T. 2012. A Methodology for Estimating Seismic Hysteretic Energy of Buildings. Civil Engineering and Urban Planning, 2012, 17-21.
- [54] Okur, A., Erberik, M.A. 2014. Adaptation of Energy Principles in Seismic Design of Turkish RC Frame Structures. Part I: Distribution of Hysteretic Energy. Proceedings of the 2nd European Conference on Earthquake Engineering and Seismology, August 25-29, Istanbul, Turkey.
- [55] Wang, F., Li, H.N., Yi, T.H. 2015. Energy Spectra of Constant Ductility Factors for Orthogonal Bidirectional Earthquake Excitations. Advances in Structural Engineering, 18(11), 1887-1899.
- [56] Akbaş, B., Akşar, B., Doran, B., Alacalı, S. 2016. Hysteretic Energy to Energy Input Ratio Spectrum in Nonlinear Systems. Dokuz Eylül University Faculty of Engineering Journal of Science and Engineering, 18(2), 239-254.
- [57] Khashaei, P. 2004. Energy-based seismic design and damage assessment for structures. Southern Methodist University, PhD Dissertation, Dallas, Texas.
- [58] PEER. 2017. Pacific Earthquake Engineering Research Center Strong Ground Motion Database. <http://ngawest2.berkeley.edu/>, (Access Date: 15.04.2017).
- [59] Sivaselvan, M.V., Reinhorn, A.M. 2000. Hysteretic Models for Deteriorating Inelastic Structures. Journal of Engineering Mechanics, 126(6), 633-640.
- [60] PRISM. 2010. A Software for Seismic Response Analysis of Single-Degree-of-Freedom-Systems. Earthquake Engineering Department of Architectural Engineering, INHA University.